

1 **Measurement report: Nitrogen Isotope ($\delta^{15}\text{N}$) Signatures of Ammonia Emissions**
2 **from Livestock Farming: Implications for Source Apportionment of Haze**
3 **Pollution**

4 Jinhan Wang¹, Zhaojun Nie¹, Yupeng Zhang¹, Xiaolei Jie^{1,2}, Haiyang Liu¹, Peng
5 Zhao^{1,2,3}, Hongen Liu^{1,2,3}

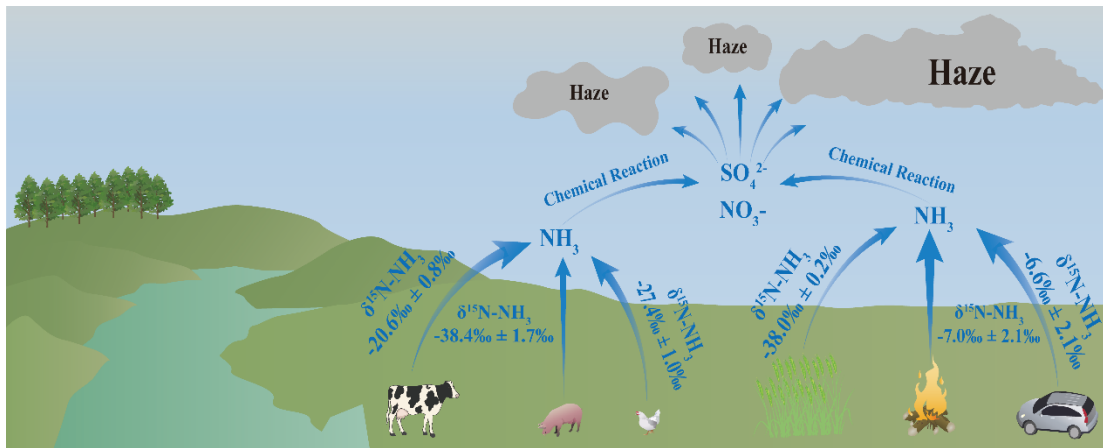
6 ¹ College of Resources and Environment, Henan Agricultural University, Zhengzhou, Henan 450046,
7 China;

8 ² Key Laboratory of Farmland Quality Conservation in the Huang-Huai-Hai Plain, Ministry of
9 Agriculture and Rural Affairs, Zhengzhou 450046, China;

10 ³ Key Laboratory of Soil Pollution Prevention, Control and Remediation in Henan Province, Zhengzhou
11 450046, China.

12 *Correspondence to:* Hongen Liu, Email: liuhongen7178@126.com; Yupeng Zhang, Email:
13 zhangyp@henau.edu.cn

14 **Abstract.** Ammonia emissions from agriculture are the primary source of atmospheric reactive nitrogen,
15 significantly impacting air pollution, soil acidification, eutrophication of water bodies, and human health.
16 Accurate quantification of ammonia from different sources is crucial for effective mitigation. In this
17 study, the air extraction method was employed to collect gases from livestock farms, and the $\delta^{15}\text{N}$ values
18 of volatilized ammonia (NH_3) from the animal husbandry industry in the southern Huang - Huai - Hai
19 Plain of China were analyzed using stable nitrogen isotopes. The results show that isotopic signatures
20 differ significantly among livestock types: dairy cows ($-20.6\text{‰} \pm 0.8\text{‰}$), laying hens ($-27.4\text{‰} \pm 1.0\text{‰}$),
21 and pigs ($-38.4\text{‰} \pm 1.7\text{‰}$). These livestock-derived signatures are distinct from those associated with
22 combustion sources ($-7.0\text{‰} \pm 2.1\text{‰}$) and traffic emissions ($6.6\text{‰} \pm 2.1\text{‰}$), and they exhibit considerably
23 lower variability than fertilizer-derived signatures. Overall, this work provides high-precision isotopic
24 source signatures for livestock operations, offering essential parameters for regional atmospheric
25 ammonia source apportionment and highlighting the need for locally tailored mitigation strategies.



26

27 Graphical Abstract.

28 1. Introduction

29 Ammonia (NH₃) is a highly reactive and abundant nitrogenous gas in the atmosphere. It is classified
 30 as a major alkaline species and readily reacts with sulfuric acid and nitric acid to produce ammonium
 31 sulfate ((NH₄)₂SO₄) and ammonium nitrate (NH₄NO₃) (Kawashima et al., 2023; Kirkby et al., 2011).
 32 These compounds can form particulate ammonium salts or interact with organic aerosols to generate
 33 secondary aerosols. In moderately polluted environments, the mass fraction of these ammonium-
 34 containing particles within PM_{2.5} is relatively low (Huang et al., 2014; Yang et al., 2011). Under severe
 35 pollution conditions, however, ammonium sulfate, ammonium nitrate, and other ammonium salts can
 36 account for up to approximately 50% of the total PM_{2.5} mass (Battye, 2003; Beusen et al., 2008; Goebes
 37 et al., 2003). As a key precursor of secondary inorganic aerosols, NH₃ is a primary contributor to haze
 38 formation and constitutes a substantial component of PM_{2.5} in polluted atmospheres (Wu et al., 2024;
 39 Xiang et al., 2022). Excessive ammonia emissions also drive a range of environmental problems,
 40 including soil acidification, climate perturbation, reduced atmospheric visibility, and eutrophication of
 41 aquatic ecosystems (Huang et al., 2012; Jiang et al., 2021). Consequently, reducing NH₃ emissions has
 42 recently been proposed as a strategy to mitigate smog pollution in China (Liu et al., 2019).

43 Over the past few decades, substantial changes in air quality have been observed across many
 44 countries worldwide (Boyle, 2017; Warner et al., 2017). Notably, China has consistently ranked first in
 45 global ammonia (NH₃) emissions (Liu et al., 2013). Current NH₃ emission inventories identify the
 46 principal sources as agricultural activities-including fertilizer application and livestock and poultry
 47 farming-and non-agricultural sources, such as combustion processes and vehicular emissions (Bouwman

48 et al., 1997; Schlesinger and Hartley, 1992; Streets et al., 2003). It is widely recognized that agriculture
49 represents the predominant source of atmospheric NH₃, contributing over 70% of total emissions (Meng
50 et al., 2017; Xu et al., 2024), accounting for more than 70% of the total (Ma et al., 2021; Ti et al., 2019),
51 with livestock and poultry farming alone accounting for 50% to 60% of agricultural NH₃ emission
52 (Huang et al., 2012; Wang et al., 2018). Despite this, substantial uncertainty remains regarding the
53 contribution of livestock-derived NH₃ to nitrogen deposition (Elliott et al., 2019), and estimating these
54 contributions using satellite remote sensing and livestock emission inventories remains challenging
55 (Beusen et al., 2008; Li et al., 2023a; Van Damme et al., 2018). These conventional approaches typically
56 rely on fixed emission factors, such as unit animal excretion coefficients, which are limited by temporal
57 lags and insufficient spatial resolution, thereby hindering the capture of real-time variations in NH₃
58 emissions and the resulting nitrogen deposition at the farm scale. In contrast, nitrogen stable isotope
59 analysis ($\delta^{15}\text{N}$) provides a direct and highly effective approach for tracing the sources of NH₃ and NH₄⁺
60 (Bhattarai et al., 2020; Xiao et al., 2020). This methodology relies on the principle that distinct emission
61 sources and environmental processes generally exhibit unique isotopic fingerprints (Elliott et al., 2019;
62 Li et al., 2024; Sui et al., 2020), defined by the ratio of heavy (¹⁵N) to light (¹⁴N) nitrogen isotopes in
63 collected samples (Song et al., 2021).

64 Numerous studies have employed stable nitrogen isotope ($\delta^{15}\text{N}$) techniques to quantify the
65 contributions of combustion, transportation, and agricultural activities to atmospheric NH₃ and NH₄⁺
66 (Xiang et al., 2022; Xie et al., 2008). For example, during the corn growing season in Northeast China,
67 $\delta^{15}\text{N}$ values of NH₃ volatilized from farmland exhibited a wide range, from -38.0‰ to -0.2‰. Notably,
68 $\delta^{15}\text{N}$ emission rates were considerably lower during the early stages of corn growth compared to later
69 stages, indicating clear seasonal variation (Song et al., 2024). Under different fertilization regimes,
70 significant differences in $\delta^{15}\text{N}$ -NH₃ emissions were observed, with values fluctuating between -46.0‰
71 and -4.7‰ throughout the volatilization period (Ti et al., 2021). Previous studies report that $\delta^{15}\text{N}$ -NH₃
72 and $\delta^{15}\text{N}$ -NH₄⁺ emissions from combustion sources (-7.6‰ to +16.2‰) predominate in winter,
73 contributing up to 51.6% of total ammonia emissions (Xiao et al., 2022, 2025; Zhou et al., 2021). In
74 contrast, NH₃ emissions from vehicle exhaust exhibit relatively high $\delta^{15}\text{N}$ values ($13.7 \pm 3.7\%$) (Savard
75 et al., 2017; Xi et al., 2023). However, these emissions are primarily localized in urban environments.

76 Currently, limited studies have reported the $\delta^{15}\text{N}$ characteristics of ammonia from livestock and
77 poultry farming. Existing data mostly rely on passive sampling methods (Berner and David Felix, 2020;

78 Chang et al., 2016; Ti et al., 2018), which assess $\delta^{15}\text{N}$ changes by collecting wet deposition samples
79 surrounding farms (pig farms: -35.1‰ to -10.5‰; cattle farms: -24.7‰ to -11.3‰). Additional research
80 has quantified $\delta^{15}\text{N}$ variability in livestock and poultry (-31.0‰ to -15.0‰) through simulated ammonia
81 emissions during manure management processes (Hristov et al., 2009). It is noteworthy that $\delta^{15}\text{N-NH}_3$
82 fluctuations in livestock and poultry operations may also depend on animal growth stages and
83 reproductive status..

84 The Bayesian stable isotope mixing model MixSAIR is primarily used to allocate contributions of
85 atmospheric emission sources through isotope analysis. MixSIAR is a stable isotope mixing model based
86 on the Bayesian statistical framework, designed to quantitatively analyze the relative contributions of
87 multiple potential sources to the isotopic composition of observed mixtures. Its fundamental assumption
88 posits that the isotopic signature of a mixture can be expressed as a linear combination of the isotopic
89 characteristics of each source weighted by their proportional contributions, while explicitly accounting
90 for source variability, measurement errors, and isotopic fractionation. (Chang et al., 2016; Walters et al.,
91 2022). However, there is no universally fixed $\delta^{15}\text{N-NH}_4^+$ value for each emission source. As a result,
92 substantial variations in reported $\delta^{15}\text{N-NH}_4^+$ values for the same source have been documented across
93 different studies. To date, no research has validated changes in $\delta^{15}\text{N-NH}_4^+$ resulting specifically from
94 livestock and poultry farm emissions, nor has the relationship between $\delta^{15}\text{N-NH}_4^+$ from different sources
95 and regional variations been examined. To obtain more accurate assessments of $\delta^{15}\text{N-NH}_3$ variations
96 associated with ammonia emissions from livestock and poultry farming, and to achieve reliable
97 atmospheric NH_3 source apportionment, it is essential to characterize the correlation between $\delta^{15}\text{N-NH}_4^+$
98 from different sources and regional differences. In this study, active dynamic sampling methods were
99 used to collect ammonia emissions from intensive pig farms, dairy farms, and laying hen farms located
100 in the southern region of the Huang-Huai-Hai Plain. Meta-analysis techniques were employed to analyze
101 the $\delta^{15}\text{N}$ signatures of different ammonia emission sources. The specific objectives of this research are:
102 (1) to determine the $\delta^{15}\text{N-NH}_4^+$ values of emissions from livestock and poultry housing at various growth
103 stages; and (2) to investigate the relationship between $\delta^{15}\text{N-NH}_4^+$ from different sources and regional
104 variations.

105 **2. Materials and methods**

106 **2.1. Sampling points in the study area and sample collection and processing.**

107 The sampling experiment at the farm was conducted from May 9, 2024, to December 6, 2024. No
108 samples were collected in July and August due to the absence of livestock or poultry during these months.
109 The collected samples covered the entire breeding period of fattening pigs and the period from chicks to
110 peak egg production in laying hens. Throughout the trial period, six batches of samples were obtained,
111 amounting to a total of 120 samples for measuring ammonia emissions from livestock and poultry
112 housing. On days when samples were collected during hazy weather, the air pollution level was classified
113 as severe, whereas samples collected under clean atmospheric conditions corresponded to air quality
114 classified as excellent. The sampling principle is based on active air sampling combined with aqueous
115 absorption. Ambient air was continuously drawn through an impinger containing deionized water, in
116 which gaseous NH_3 was absorbed and converted to dissolved NH_4^+ . After sampling, the absorption
117 solution was quantitatively recovered for subsequent laboratory analysis. Under the applied sampling
118 flow rate and duration, the method detection limit for atmospheric NH_3 was on the order of 3 ppb, which
119 is adequate for resolving ambient concentration variations during the observation period. Potential
120 interferences include the co-collection of particulate NH_4^+ and the absorption of other water-soluble
121 alkaline gases. These effects were minimized by controlled sampling duration, appropriate flow rates,
122 and blank correction procedures, and are considered to have a negligible influence on the measured NH_3
123 concentrations. Samples were collected using atmospheric samplers (Beijing Ke'an Labor Protection
124 Company) at a flow rate of 0.1 to 2 $\text{L}\cdot\text{min}^{-1}$, with each sample collected over a duration of 60 minutes
125 (Ferm, 1979; Harrison and Kitto, 1990; Heaton, 1986). All NH_3 samples were collected at a constant and
126 identical flow rate throughout the study period, with all flow rates complying with the National Standard
127 GB 3095-2012.

128 The intensive fattening pig farm is located in Luoyang City, Henan Province (112.71° E, 34.52° N),
129 with no other livestock operations in the surrounding area. The sampled fattening pig farm houses 2,600
130 pigs distributed across four fully enclosed pig houses. One of these houses was selected as the target
131 sampling site. The sampling procedure was as follows: an atmospheric sampler was positioned 2.0 meters
132 from the exhaust vent of the livestock and poultry house at a height of 1.6 meters, corresponding to the
133 central height of the exhaust outlet. The sampling duration was set to 60 minutes, with the gas flow rate

134 maintained at $2 \text{ L} \cdot \text{min}^{-1}$ using a flow meter. According to the sample requirements for mass spectrometry
135 pretreatment, we used deionized water as the absorption solution. A bubbler absorption bottle filled with
136 absorption solution was used to collect NH_3 . Three atmospheric samplers were operated simultaneously
137 during each sampling event. Figure 1 marks the sampling points of the intensive pig farms with green
138 pentagrams. Sampling was conducted in a typical commercial intensive laying-hen house with a
139 conventional cage-based rearing system, representative of large-scale laying-hen farms in northern China.
140 We collected gases from the exhaust vents of chicken houses and pig houses. These types of animal
141 housing have centralized air inlets and outlets, so collecting from the exhaust vents can represent the
142 ammonia emissions from these two types of housing into the atmosphere. For cattle farms, since the
143 barns are open, we selected cattle sheds located in the middle of the farm to more effectively collect
144 ammonia gas.

145 In the case of intensive laying hens farms, each building houses approximately 15,000 laying hens
146 and is fully enclosed, with a total of 300,000 laying hens being raised. The sampling site is located in
147 Zhengzhou City, Henan Province (114.03° E , 34.59° N). One building was selected as the target sampling
148 point, with the sampling method mirroring that used for the fattening pig farms. As shown in Figure 1,
149 the light blue pentagons represent the sampling points of intensive layer farms.

150 The intensive dairy farm operates with an open-style barn design, housing 400 dairy cows per barn,
151 with a total of 4,000 dairy cows being raised. Four atmospheric samplers were installed in the
152 passageways of the dairy barns, with each sampler spaced 10 meters apart and positioned at a height of
153 1.6 meters. The dairy farm is located in Zhengzhou City, Henan Province (114.11° E , 34.81° N). The
154 sampling time and method remained consistent with those described above. In Figure 1, the dark blue
155 pentagons represent the sampling points of intensive dairy farms.

156 To investigate the variations in $\delta^{15}\text{N}$ levels associated with differing degrees of air pollution, samples
157 collected for $\delta^{15}\text{N}$ measurement during periods of severe smog and when air quality was pristine. The
158 sampling location was situated on a spacious lawn within the campus of Henan Agricultural University,
159 devoid of tall buildings or traffic. The sampling point is illustrated in Figure 1, where the pink triangle
160 represents the sampling site for both haze and clean air (Longitude 113.82° E , Latitude 34.80° N). Each
161 sampling event utilized three atmospheric samplers, positioned at a height of 1.6 meters, with the duration
162 of sampling aligned with that of the livestock farm.

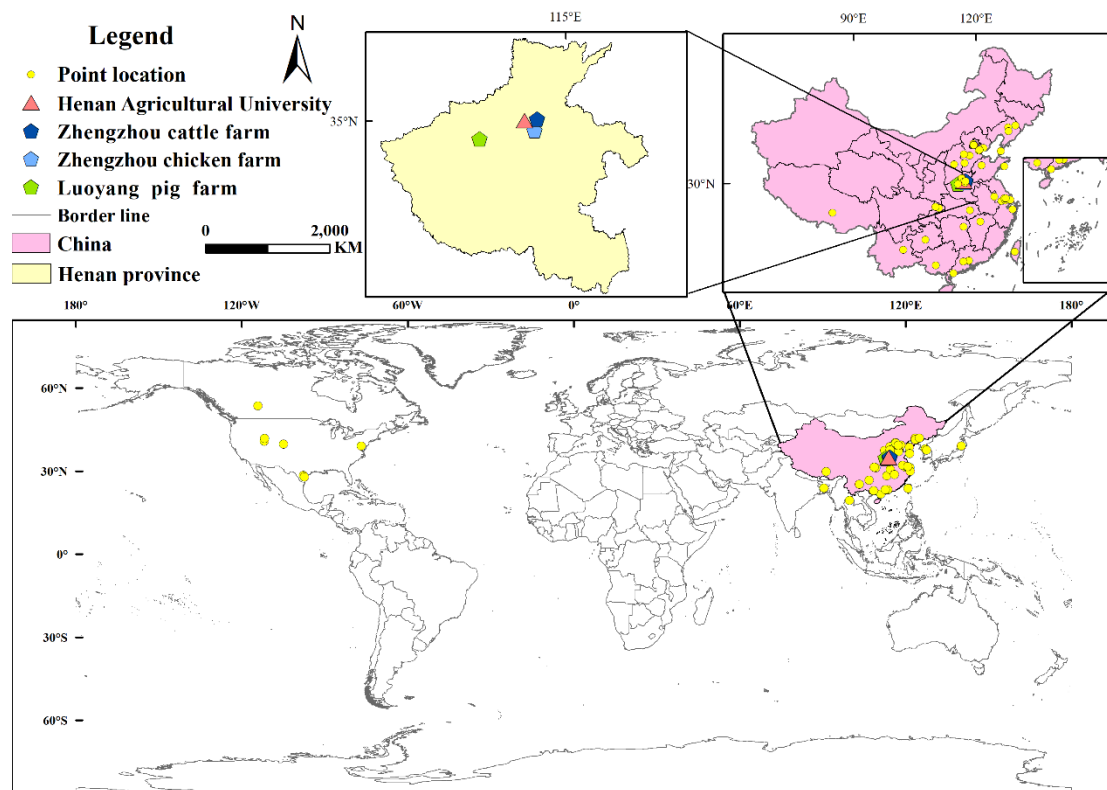
163 The collected sample solution is transferred into a centrifuge tube and returned to the laboratory,

164 where the concentration of NH_3 is measured using a UV spectrophotometer. The detection method
165 adheres to the guidelines outlined in “Determination of Ammonia Nitrogen in Water by Salicylic Acid
166 Spectrophotometry” (HJ 536-2009), and the calculation method is presented in Equation (1):

$$167 \quad \rho_N = \frac{A_s - A_b - a}{b \times V} \times D \quad (1)$$

168 Where, ρ_N represents the mass concentration of ammonia nitrogen in the water sample (expressed as N),
169 in $\text{mg} \cdot \text{L}^{-1}$. The variables are defined as follows: A_s denotes the absorbance of the sample, while A_b
170 indicates the absorbance of the blank experiment, which is prepared from the same batch as the sample.
171 The parameters a and b correspond to the intercept and slope of the calibration curve, respectively.
172 Additionally, V refers to the volume of the water sample taken, measured in mL, and D signifies the
173 dilution factor of the water sample.

174 The analytical method for N isotope determination employs the hypobromite-hydroxylamine
175 hydrochloride chemical method (Song et al., 2024) (Soler-Jofra et al., 2016; Zhang et al., 2007). Initially,
176 a potassium bromate-potassium bromide solution reacts under acidic conditions to produce bromine,
177 which subsequently reacts in a strongly alkaline environment to generate bromate, a potent oxidizing
178 agent capable of oxidizing NH_4^+ to NO_2^- . In the following step, hydroxylamine hydrochloride reduces
179 NO_2^- in an acidic environment to form N_2O . The resultant N_2O is then analyzed using a stable isotope
180 ratio mass spectrometer, along with a multi-purpose online gas preparation device, and an automatic
181 sampler, to determine the $\delta^{15}\text{N}$ value. For each sample analysis, four international standard materials for
182 NH_4^+ (IAEA-N-1, USGS-25, IAEA-N-2, and USGS-26, with $\delta^{15}\text{N}$ concentrations of 0.4‰, -30.41‰,
183 20.3‰, and 53.75‰, respectively) are processed simultaneously. NH_3 concentrations and $\delta^{15}\text{N}$ values
184 are presented as mean \pm standard error (SE). Differences in $\delta^{15}\text{N}$ values among livestock categories were
185 evaluated using one-way analysis of variance (ANOVA). When data did not meet the assumptions of
186 normality or homogeneity of variance, non-parametric tests were applied. Statistical significance was
187 defined at $p < 0.05$. All statistical analyses were conducted using standard statistical software.



188

189 Figure 1. Sampling sites of livestock farms, haze weather, and clear weather in this study, extracted from
 190 the main research sampling locations. Yellow dots represent the main global research sampling sites, pink
 191 triangles represent sampling sites during haze and clear weather, dark blue pentagons represent cattle
 192 farms, light blue pentagons represent layer farms, and green pentagons represent fattening pig farms.

193 **2.2. Data collection and processing**

194 We screened articles published between January 2000 and January 2025 regarding the sources of
 195 $\delta^{15}\text{N-NH}_3$ and $\delta^{15}\text{N-NH}_4^+$. Specifically, we utilized ISI Web of Science, Google Scholar, and PubMed,
 196 employing the search terms “ $\delta^{15}\text{N}$,” “ NH_3 ,” “ammonia emissions,” and “isotopes” to identify relevant
 197 literature. Studies included in our analysis were required to meet the following criteria: (1) Samples must
 198 be measured for either $\delta^{15}\text{N-NH}_3$ or $\delta^{15}\text{N-NH}_4^+$; (2) Experiments must encompass at least one of the
 199 following: combustion, fertilization, agriculture, transportation, or livestock farming; (3) The number of
 200 experimental replicates and sampling events must be explicitly reported; (4) Samples must primarily
 201 consist of atmospheric NH_3 or $\text{PM}_{2.5}$, and detection must employ chemical methods. A total of 37
 202 documents were included in the analysis. This dataset comprehensively encompasses multiple meta-
 203 analyses and original studies, detailing changes in $\delta^{15}\text{N-NH}_3$ and $\delta^{15}\text{N-NH}_4^+$ from combustion sources,
 204 transportation sources, agricultural sources, and livestock farming sources; the proportion of $\delta^{15}\text{N}$ values

205 in the atmosphere; geographical location (latitude and longitude); and the GDP of each city where
206 samples were collected. If the data in the literature was presented solely in chart form, we utilized
207 WebPlotDigitizer-4.7 (<https://apps.automeris.io/wpd4/>) to extract the data. We categorized the collected
208 data into five distinct groups: combustion, transportation, farmland, livestock farming, and PM_{2.5}. To
209 ensure reproducibility, literature-derived $\delta^{15}\text{N-NH}_3$ values were synthesized following a consistent
210 aggregation protocol. When multiple isotopic values for the same source category were reported within
211 a single study, a sample-size-weighted mean was calculated if the number of samples (n) was explicitly
212 provided. In cases where sample size information was unavailable, simple arithmetic means were used,
213 and the resulting uncertainty was reflected by expanding the reported end-member range. No additional
214 weighting based on study duration or subjective data quality scores was applied, in order to avoid
215 introducing implicit bias across studies. Differences between sampling methodologies were explicitly
216 considered. Active sampling studies, including the present work, were prioritized for constraining source
217 end-member values. Passive sampling data were used only for qualitative comparison, as previous
218 studies have demonstrated systematic low biases in $\delta^{15}\text{N-NH}_3$ derived from passive samplers relative to
219 active methods. Consequently, passive sampling results were not directly incorporated into end-member
220 mean calculations used for isotope mixing analyses.

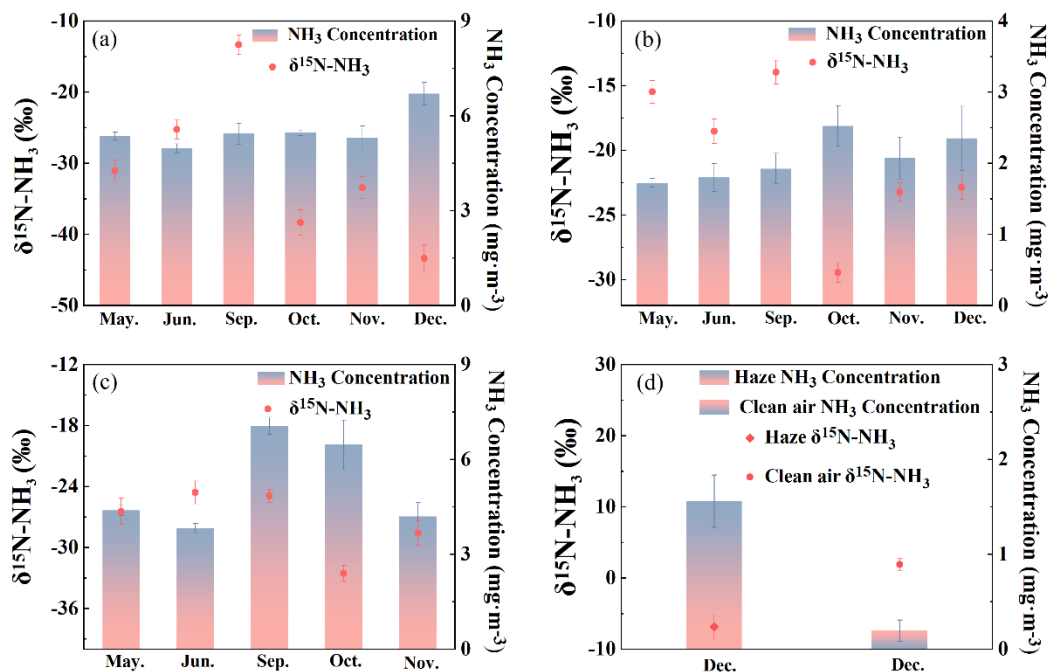
221 A total of 126 samples were collected, and 41 literature references were gathered. Data analysis was
222 performed using Excel, SPSS, and Python version 3.11.

223 **3. Result and discussion**

224 **3.1. Temporal Variations in Ammonia Emissions and $\delta^{15}\text{N}$ Signatures from Livestock Farms**

225 During the sampling period from May to December, ammonia emissions varied significantly among
226 the three farm types: 4.9 to 6.7 mg·m⁻³ for fattening pigs (Figure 2a), 1.7 and 2.5 mg·m⁻³ for dairy cows
227 (Figure 2b), and 3.8 to 7.1 mg·m⁻³ for laying hens (Figure 2c), with the latter exhibiting substantial
228 temporal fluctuations. NH₃ emissions from fattening pigs peaked when the pigs reached 130 kg·head⁻¹
229 (Figure 2a). For laying hens, NH₃ concentrations initially increased and subsequently declined in
230 response to temperature variations, reflecting enhanced urease activity within the housing environment,
231 which accelerates urea hydrolysis and promotes NH₃ volatilization. $\delta^{15}\text{N-NH}_4^+$ levels at the livestock
232 farms showed significant temporal variation ($p < 0.05$) (Groot Koerkamp et al., 1998; Rosa et al., 2020).

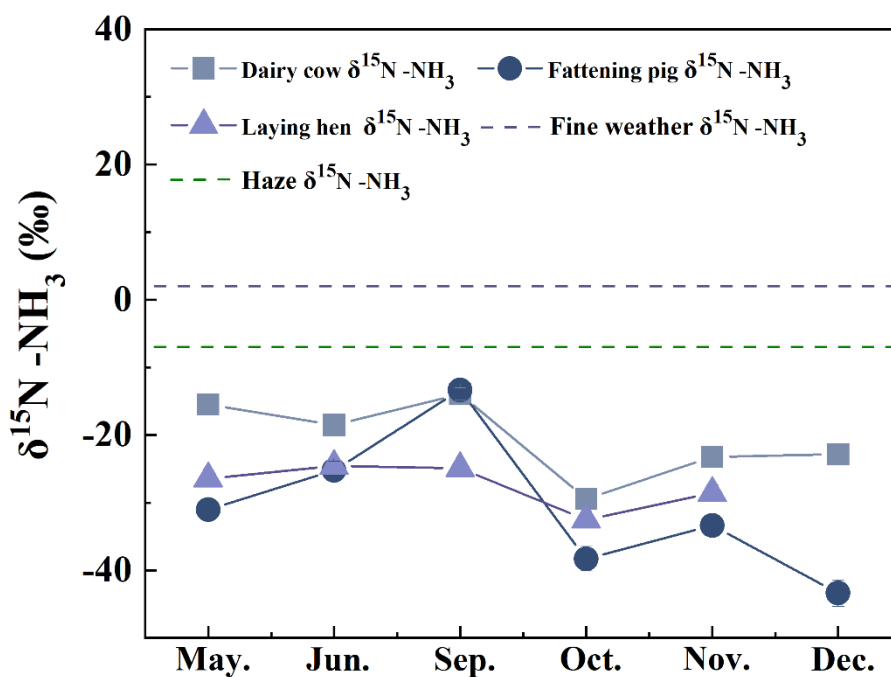
233 From May to June, the $\delta^{15}\text{N-NH}_4^+$ increased from -31.0‰ to -25.2‰ in fattening pig farms and from -
 234 26.4‰ to -24.6‰ in laying hen farms. In September, $\delta^{15}\text{N-NH}_4^+$ values from fattening pig farms (-13.3
 235 ± 1.3 ‰) were significantly higher than those from laying hen and dairy cow farms (-13.9 ± 0.9 ‰), which
 236 were comparable. Over the following three months, $\delta^{15}\text{N-NH}_4^+$ levels decreased significantly across both
 237 farm types. Although relatively large variability was observed within each livestock category, the
 238 differences in mean $\delta^{15}\text{N}$ values among groups were statistically significant (one-way ANOVA, $p <$
 239 0.05). The large within-group variability reflects realistic operational and environmental heterogeneity
 240 and does not negate the statistically significant differences observed among livestock categories. As
 241 illustrated in Figure 2, the highest NH_3 concentration at the dairy farm ($2.5 \pm 0.3 \text{ mg}\cdot\text{m}^{-3}$) occurred in
 242 October, coinciding with the lowest $\delta^{15}\text{N-NH}_4^+$ values. while laying hen farms also recorded minimum
 243 $\delta^{15}\text{N-NH}_4^+$ during this period of elevated NH_3 . Conversely, the lowest $\delta^{15}\text{N-NH}_4^+$ at fattening pig farms
 244 was observed in December, despite peak NH_3 concentrations. NH_3 concentrations differed significantly
 245 between hazy and clear weather in December (Figure 2d), with $\delta^{15}\text{N-NH}_4^+$ values being significantly
 246 higher under clear conditions (1.9 ± 0.8 ‰) than under hazy conditions (1.6 ± 0.2 ‰; $p < 0.05$).



247
 248 Figure 2. Changes in NH_3 emissions and $\delta^{15}\text{N-NH}_4^+$ values outside the livestock farms among different
 249 months. (a) Fattening pig farm; (b) Dairy cow farm; (c) Laying hens farm; (d) Comparison of Haze and
 250 clean air samples. Statistical difference was calculated by T-test, $P < 0.05$, $n = 3$.

251 As illustrated in Figure 3, throughout the entire monitoring period, ammonia (NH_3) sources form

252 the farms exhibited nitrogen depletion, indicated by negative $\delta^{15}\text{N-NH}_4^+$ values. Overall, $\delta^{15}\text{N-NH}_4^+$
 253 values exhibited significant fluctuations in dairy and fattening pig farms, while variations were
 254 comparatively moderate in laying hens farms. Notably, the $\delta^{15}\text{N-NH}_4^+$ values at dairy cattle farms
 255 displayed substantially greater overall changes during the monitoring period compared to those in laying
 256 hens and fattening pig farms. The arithmetic mean value at fattening pig farms was $-30.8 \pm 1.6\%$, the
 257 lowest among the three types of farms, whereas the $\delta^{15}\text{N-NH}_4^+$ values in laying hens manure remained
 258 at an intermediate level throughout the entire period. From October to December, the $\delta^{15}\text{N-NH}_4^+$ values
 259 at livestock and poultry farms were generally lower than those observed in the first half of the monitoring
 260 period (Figure 3). However, when comparing hazy and clear weather conditions, the $\delta^{15}\text{N-NH}_4^+$ values
 261 for all three types of farms consistently remained at a relatively low level during this timeframe (Figure
 262 3). High temperatures enhance enzyme activity and volatilization, thereby intensifying the isotopic
 263 fractionation effect during summer; whereas low temperatures inhibit these processes and reduce isotopic
 264 deviations. The nitrogen isotopic signature of livestock-derived ammonia is influenced by various
 265 biogeochemical processes, including urea hydrolysis during manure storage, microbial ammonification,
 266 and ammonia volatilization (Bhattarai and Wang, 2023; Huang et al., 2012; Li et al., 2023a).



267

268 Figure 3. Changes of $\delta^{15}\text{N-NH}_4^+$ abundance at intensive livestock farms during the sampling period. Hazy

269 and clean air were also sampled at December. The air sample of laying hens in December was missed,
270 because of death of chicken by avian influenza.

271 **3.2. Comparison with Literature and Implications for Local Sources**

272 During the monitoring period, the $\delta^{15}\text{N-NH}_4^+$ values ranged from -50.0‰ to -10.0‰ (Figure 4a).
273 For fattening pigs, $\delta^{15}\text{N-NH}_4^+$ values averaged $-38.4\text{‰} \pm 1.8\text{‰}$ between October and December, which
274 was significantly lower than the previously reported range of -27.10‰ to -31.7‰ (Chang et al., 2016)
275 Notably, the overall variation remained within the $\delta^{15}\text{N-NH}_4^+$ emission ranges report for fattening pigs
276 in other studies (Bhattarai and Wang, 2023; Wang et al., 2022). Furthermore, due to differences in
277 livestock management practices and nitrogen content in feed, the $\delta^{15}\text{N-NH}_4^+$ values from dairy farms in
278 this study, averaging $-29.4\text{‰} \pm 13.9\text{‰}$, were substantially lower than those reported by Martine et al.
279 ($20.5\text{‰} \pm 34.5\text{‰}$) (Savard et al., 2017).

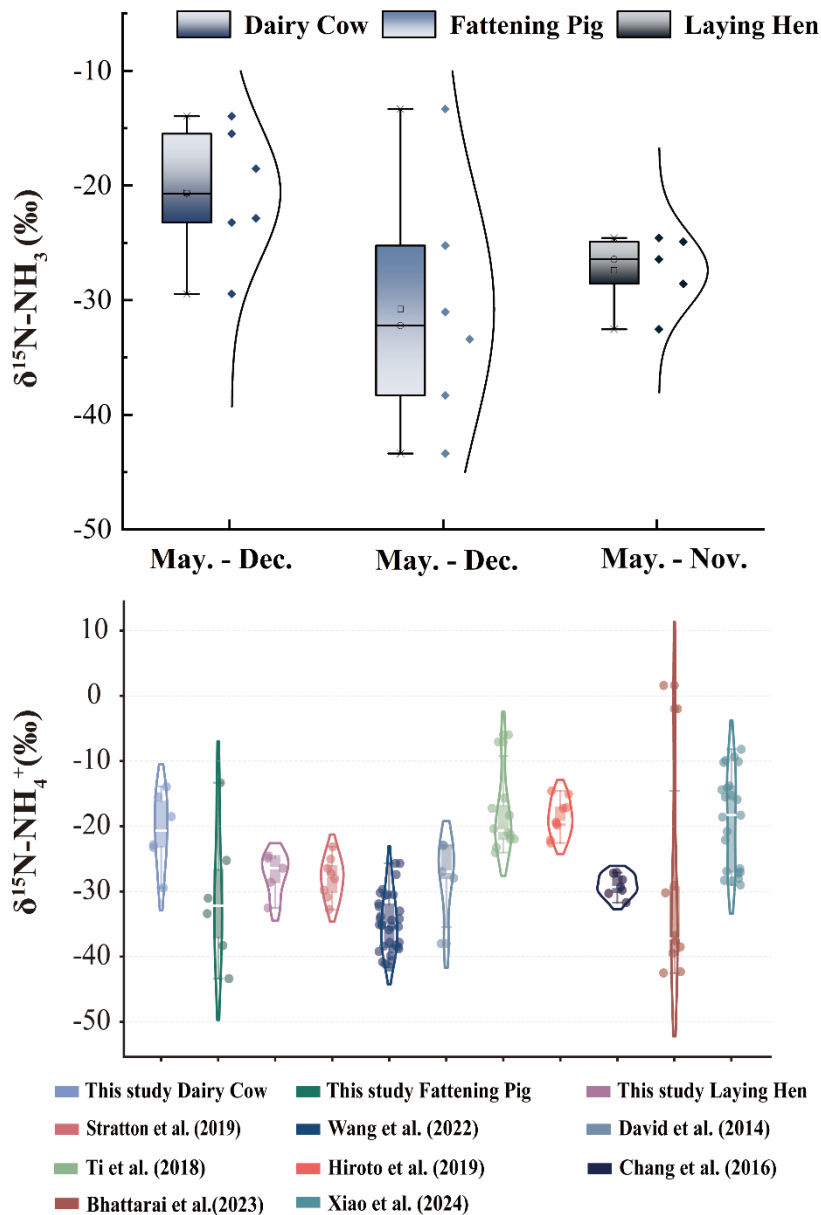
280 Comparison with $\delta^{15}\text{N-NH}_4^+$ values measured in dairy farms in Akita, Japan, were $-22.5\text{‰} \pm 14.6\text{‰}$
281 (Kawashima, 2019), no significant difference was observed relative to the values obtained in this study.
282 However, these values exceeded those reported by David et al. (Felix et al., 2014), which ranged from -
283 37.9‰ to -22.9‰ based on passive sampling techniques. Previous research has shown that active
284 sampling generally yields higher $\delta^{15}\text{N}$ values than passive sampling (Kawashima and Ono, 2019; Pan et
285 al., 2020). This discrepancy arises from the diffusion-driven nature of passive samplers, in which lighter
286 NH_3 molecules are preferentially adsorbed. Consequently, passive sampling typically produces $\delta^{15}\text{N}$
287 values that deviate by approximately 15‰ from those obtained by active sampling (Bhattarai and Wang,
288 2023; Skinner et al., 2006). Variations in $\delta^{15}\text{N-NH}_4^+$ values are known to occur among different livestock
289 species. During the monitoring period, $\delta^{15}\text{N-NH}_4^+$ values from laying hen farms were consistently lower
290 than those from dairy farms but higher than those from fattening pig farms, consistent with previously
291 reported trends (Liu et al., 2025; Ryu et al., 2021). This pattern suggests that $\delta^{15}\text{N-NH}_4^+$ variations in
292 emitted NH_3 are not primarily driven by animal body weight but are instead strongly modulated by
293 environmental conditions (Choi et al., 2017; Qu and Zhang, 2021). In agreement with earlier studies,
294 $\delta^{15}\text{N-NH}_4^+$ emissions from fattening pig and laying hen farms differed significantly from previously
295 documented values, whereas no significant difference was observed for dairy cattle farms. Furthermore,
296 the magnitude of $\delta^{15}\text{N-NH}_4^+$ fluctuations across the three farm types was smaller than that reported in
297 earlier literature. Comparison with major atmospheric NH_3 sources further demonstrated that the $\delta^{15}\text{N-NH}_4^+$

298 NH_4^+ values measured in this study diverged substantially from those associated with combustion (-7.0%
299 $\pm 2.1\%$), fertilization application ($-38.0\% \pm 0.2\%$), and transportation ($6.6\% \pm 2.1\%$). Based on $\delta^{15}\text{N}$ -
300 NH_4^+ signatures measured under both hazy and clear weather conditions, it can therefore be inferred that
301 agricultural and livestock emissions are not the dominant contributors to atmospheric NH_3 in Zhengzhou.
302 Instead, traffic exhaust and combustion sources appear to constitute the primary contributors. We
303 conducted source apportionment for haze and clean weather using the MixSIAR model. The results
304 showed that combustion+n and traffic were the main contributing sources, with combustion accounting
305 for 29.0%, traffic for 38.0%, agriculture for 15.1%, and livestock for 17.8% (Stock and Semmens, 2016;
306 Walters et al., 2022; Wong et al., 2022).

307 The selected pig, dairy, and laying hen facilities are typical of intensive livestock production systems
308 in the southern Huang–Huai–Hai Plain, where feeding strategies, manure management, and ventilation
309 designs are relatively standardized due to regional regulations and industrial practices. Previous studies
310 have shown that while such operational differences can induce secondary variability in $\delta^{15}\text{N}$ signatures,
311 their influence is generally smaller than the systematic isotopic contrasts observed among different
312 livestock species.

313 Importantly, the objective of this study is not to characterize farm-to-farm variability, but to
314 constrain representative isotopic end-member ranges for major livestock categories that can be applied
315 in regional source apportionment frameworks. Within this context, the internally consistent sampling
316 protocol and the clear separation of $\delta^{15}\text{N}$ - NH_4^+ values among livestock types suggest that the derived
317 signatures are robust for intensive livestock systems operating under comparable management conditions
318 (Choi et al., 2017; Parnell et al., 2010).

319 Extrapolation of these $\delta^{15}\text{N}$ signatures beyond the studied region or to non-standardized, small-scale,
320 or pasture-based livestock systems should be undertaken with caution. Future work incorporating
321 multiple facilities per livestock type and explicit characterization of feed and ventilation parameters
322 would further refine the regional representativeness of livestock-derived ammonia isotope signatures.



323

324 Figure 4. Comparison of $\delta^{15}\text{N-NH}_4^+$ values within different livestock farms and historical reported data.

325 (a) Comparison of the $\delta^{15}\text{N-NH}_4^+$ values among different livestock farms; (b) Comparison of the $\delta^{15}\text{N-NH}_4^+$

326 NH_4^+ values from present study with previously reported data. Boxes represent the interquartile range,

327 the horizontal line within each box denotes the median value, and whiskers indicate the minimum and

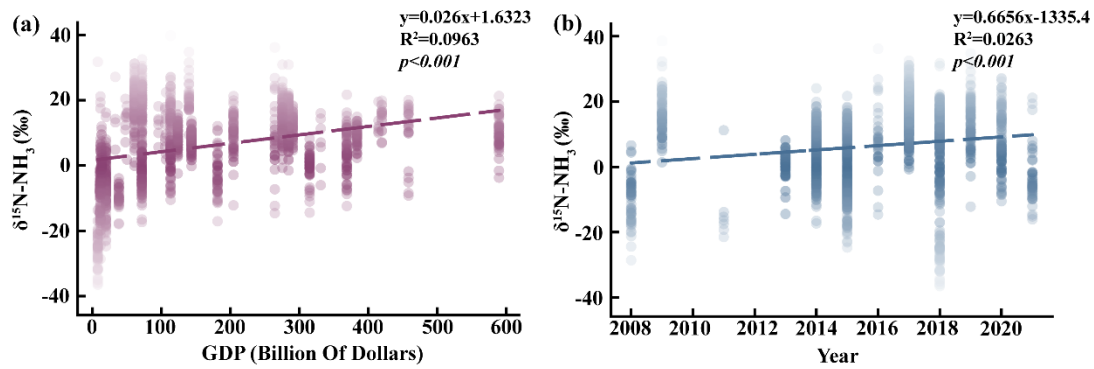
328 maximum values excluding outliers. Individual points outside the whiskers represent statistical outliers.

329 3.3. Global Variability of NH_3 Source Signatures and Challenges for Source Apportionment

330 Ammonia emissions that contribute to urban smog primarily arise from combustion activities,

331 vehicle exhaust, agriculture fertilization, and livestock production. As national economies expand, the
332 frequency and severity of smog events have intensified. Figure 5a (slope: 0.026, intercept: 1.6323, R^2 :
333 0.0963) shows that from 2000 to 2025, when GDP remains below 70 billion USD, atmospheric $\delta^{15}\text{N}$ -
334 NH_4^+ signatures predominantly reflect fertilizer-derived emissions from agricultural regions and NH_3
335 volatilization from livestock operations (Kawashima et al., 2022; Kawashima and Kurahashi, 2011). This
336 pattern indicates that lower-income regions rely heavily on agriculture and animal husbandry as the
337 foundational components of their economies (Leng et al., 2018).

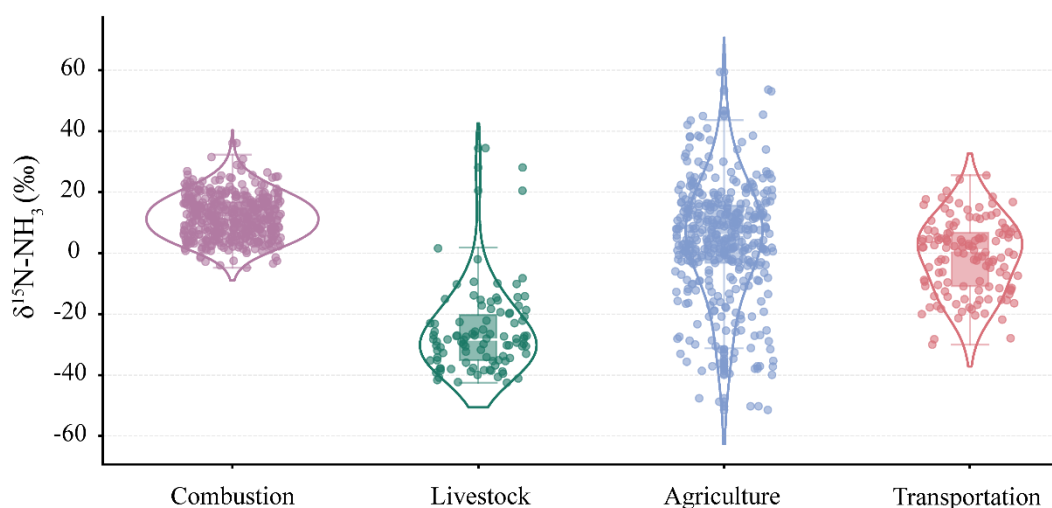
338 When GDP increases to between 80 billion and 300 billion USD, the contribution of combustion-
339 related and vehicular sources to $\delta^{15}\text{N}$ - NH_4^+ becomes increasingly prominent. Notably, vehicle exhaust
340 remains the dominant contributor within this GDP interval, suggesting that transportation serves as a key
341 economic driver during mid-stage development. In densely populated and economically advanced cities,
342 rapid vehicle growth further amplifies the influence of transportation-related $\delta^{15}\text{N}$ - NH_4^+ signatures (Lim
343 et al., 2022; Pan et al., 2018; Stratton et al., 2019). Throughout the entire dataset, vehicle exhaust and
344 combustion together account for nearly 70% of ammonia emissions (Wu et al., 2019). Once GDP
345 surpasses 300 billion USD, $\delta^{15}\text{N}$ - NH_4^+ from combustion becomes the dominant atmospheric source,
346 while the relative contribution from vehicle exhaust begins to decline and emissions from agricultural
347 fertilization and livestock farming become negligible (Li et al., 2023b). It is important to note that
348 sampling sites in the present study were located near power plants (Lim et al., 2019; Zou et al., 2022),
349 whereas comparison data from previous studies were collected in urban cores. This spatial difference
350 further supports the conclusion that in highly developed cities, shifts in economic structure lead to
351 combustion sources emerging as the principal contributors to atmospheric NH_3 under both hazy and clear
352 meteorological conditions. As illustrated in Figure 5b, the proportion of $\delta^{15}\text{N}$ - NH_4^+ attributed to
353 combustion and vehicular sources has increased over time. This temporal trend suggests that, with
354 economic growth, agricultural and livestock emissions no longer represent the dominant contributors to
355 atmospheric ammonia.



356

357 Figure 5. Changes of $\delta^{15}\text{N-NH}_4^+$ values among different GDP cities and years. (a) The relationship
 358 between GDP and $\delta^{15}\text{N-NH}_4^+$ values ($p<0.001$); (b) Changes of $\delta^{15}\text{N-NH}_4^+$ values reported between 2008
 359 to 2021 ($p<0.001$).

360 The extracted dataset was classified into four major emission categories-livestock farming,
 361 combustion, farmland fertilization, and vehicle exhaust-and subsequently subjected to statistical
 362 evaluation. As illustrated in Figure 6, $\delta^{15}\text{N-NH}_4^+$ values associated with combustion sources showed
 363 strong consistency with previously reported ranges (Chang et al., 2021). Although traffic exhaust and
 364 livestock-related $\delta^{15}\text{N-NH}_4^+$ values exhibited moderate dispersion, both sources remained within
 365 relatively well-defined isotopic ranges. In sharp contrast, $\delta^{15}\text{N-NH}_4^+$ signatures following farmland
 366 fertilization displayed pronounced heterogeneity, covering nearly the entire isotopic spectrum reported
 367 for combustion, livestock, and vehicular emissions. This extensive variability highlights substantial
 368 regional differences in agricultural ammonia emission processes (Felix et al., 2014; Li et al., 2023b).
 369 Consequently, accurate source apportionment of atmospheric NH_3 requires distinguishing dominant local
 370 emission pathways rather than relying solely on generalized isotopic patterns (Chen et al., 2022; Zhang
 371 et al., 2023).



372

373 Figure 6. Statistical analysis of extracted data categorized by source: combustion sources, livestock and
 374 poultry farming sources, agricultural sources, and transportation exhaust sources. Boxes represent the
 375 interquartile range, the horizontal line within each box denotes the median value, and whiskers indicate
 376 the minimum and maximum values excluding outliers. Individual points outside the whiskers represent
 377 statistical outliers.

378 4. Summary

379 This study establishes high-precision $\delta^{15}\text{N}$ signatures for ammonia emissions from three dominant
 380 intensive livestock systems in the Huang-Huai-Hai Plain. Distinct isotopic fingerprints were identified
 381 for dairy operations ($-20.6\text{‰} \pm 0.8\text{‰}$), laying hen facilities ($-27.4\text{‰} \pm 1.0\text{‰}$), and fattening pig farms ($-$
 382 $38.4\text{‰} \pm 1.7\text{‰}$), underscoring clear differences among livestock categories. Our results further
 383 demonstrate that isotopic signatures vary dynamically with NH_3 volatilization intensity, highlighting the
 384 need to incorporate volatilization-driven fractionation effects into isotope-based source apportionment
 385 frameworks. When compared with ambient $\delta^{15}\text{N-NH}_4^+$ measurements in Zhengzhou, the newly
 386 constrained source end-members indicate that non-agricultural sources-particularly vehicular emissions
 387 and combustion-are likely major contributors to urban atmospheric ammonia. This interpretation,
 388 however, requires validation through comprehensive isotopic mixing and dispersion modeling. Moreover,
 389 global-scale evaluation reveals that the exceptional variability of $\delta^{15}\text{N}$ associated with fertilized soils
 390 continues to pose a substantial challenge for accurate identification of agricultural contributions.

391 Collectively, the findings presented here provide critical isotopic constraints that can enhance regional
392 atmospheric chemistry models and support the design of more precise and effective ammonia emission
393 control policies.

394 **Author Contributions**

395 J.W. Drafting, Formal Analysis, Data Management, Methodology, Investigation; Z.N. Formal Analysis,
396 Data Management, Methodology, Investigation; Y.Z. Conceptualization, Data Management,
397 Visualization, Funding Acquisition, Drafting, Formal Analysis, Writing - Review & Editing; X.J. Data
398 Management, Visualization; H.L. Data Management, Methodology; P.Z. Formal Analysis, Data
399 Management; H.L. Writing - Review & Editing, Funding Acquisition, Conceptualization, Supervision.

400 **Competing interest**

401 The authors declare that they have no known competing financial interests or personal relationships that
402 could have influenced the work reported in this paper.

403 **Acknowledgments.** This research was supported by the National Key Research and Development
404 Program of China (2021 YFD 1700900), the Industrial Technology System for Cultivated Land
405 Protection in Henan Province (HARS-22-19-S), the Natural Science Foundation of Henan Province
406 (Grant No. 252300420043), and the Key Research and Development Program of Henan Province (Grant
407 No. 251111112200).

408 **Data availability**

409 All data are available in the text, Supplement or publicly on Zenodo (DOI [10.5281/zenodo.17639507](https://doi.org/10.5281/zenodo.17639507)).

410 **References:**

411 Battye, W.: Evaluation and improvement of ammonia emissions inventories, *Atmos. Environ.*, 37,
412 3873–3883, [https://doi.org/10.1016/S1352-2310\(03\)00343-1](https://doi.org/10.1016/S1352-2310(03)00343-1), 2003.

413 Berner, A. H. and David Felix, J.: Investigating ammonia emissions in a coastal urban airshed using
414 stable isotope techniques, *Sci. Total Environ.*, 707, 134952,
415 <https://doi.org/10.1016/j.scitotenv.2019.134952>, 2020.

416 Beusen, A. H. W., Bouwman, A. F., Heuberger, P. S. C., Van Drecht, G., and Van Der Hoek, K. W.:
417 Bottom-up uncertainty estimates of global ammonia emissions from global agricultural production
418 systems, *Atmos. Environ.*, 42, 6067–6077, <https://doi.org/10.1016/j.atmosenv.2008.03.044>, 2008.

419 Bhattarai, N. and Wang, S.: Active vs. passive isotopic analysis: insights from urban beijing field
420 measurements and ammonia source signatures, *Atmos. Environ.*, 314, 120079,
421 <https://doi.org/10.1016/j.atmosenv.2023.120079>, 2023.

422 Bhattarai, N., Wang, S., Xu, Q., Dong, Z., Chang, X., Jiang, Y., and Zheng, H.: Sources of gaseous
423 NH₃ in urban beijing from parallel sampling of NH₃ and NH₄⁺, their nitrogen isotope measurement
424 and modeling, *Sci. Total Environ.*, 747, 141361, <https://doi.org/10.1016/j.scitotenv.2020.141361>,
425 2020.

426 Bouwman, A. F., Lee, D. S., Asman, W. a. H., Dentener, F. J., Van Der Hoek, K. W., and Olivier, J.
427 G. J.: A global high-resolution emission inventory for ammonia, *Glob. Biogeochem. Cycles*, 11,
428 561–587, <https://doi.org/10.1029/97GB02266>, 1997.

429 Boyle, E.: Nitrogen pollution knows no bounds, *Science*, 356, 700–701,
430 <https://doi.org/10.1126/science.aan3242>, 2017.

431 Chang, Y., Liu, X., Deng, C., Dore, A. J., and Zhuang, G.: Source apportionment of atmospheric
432 ammonia before, during, and after the 2014 APEC summit in beijing using stable nitrogen isotope
433 signatures, *Atmospheric Chem. Phys.*, 16, 11635–11647, [https://doi.org/10.5194/acp-16-11635-](https://doi.org/10.5194/acp-16-11635-2016)
434 2016, 2016.

435 Chang, Y., Zhang, Y.-L., Kawichai, S., Wang, Q., Van Damme, M., Clarisse, L., Prapamontol, T.,
436 and Lehmann, M. F.: Convergent evidence for the pervasive but limited contribution of biomass
437 burning to atmospheric ammonia in peninsular southeast Asia, *Atmospheric Chem. Phys.*, 21, 7187–
438 7198, <https://doi.org/10.5194/acp-21-7187-2021>, 2021.

439 Chen, T.-Y., Chen, C.-L., Chen, Y.-C., Chou, C. C.-K., Ren, H., and Hung, H.-M.: Source
440 apportionment and evolution of N-containing aerosols at a rural cloud forest in taiwan by isotope
441 analysis, *Atmospheric Chem. Phys.*, 22, 13001–13012, <https://doi.org/10.5194/acp-22-13001-2022>,
442 2022.

443 Choi, W.-J., Kwak, J.-H., Lim, S.-S., Park, H.-J., Chang, S. X., Lee, S.-M., Arshad, M. A., Yun, S.-
444 I., and Kim, H.-Y.: Synthetic fertilizer and livestock manure differently affect δ¹⁵N in the
445 agricultural landscape: a review, *Agric. Ecosyst. Environ.*, 237, 1–15,
446 <https://doi.org/10.1016/j.agee.2016.12.020>, 2017.

447 Elliott, E. M., Yu, Z., Cole, A. S., and Coughlin, J. G.: Isotopic advances in understanding reactive
448 nitrogen deposition and atmospheric processing, *Sci. Total Environ.*, 662, 393–403,
449 <https://doi.org/10.1016/j.scitotenv.2018.12.177>, 2019.

450 Felix, J. D., Elliott, E. M., Gish, T., Maghirang, R., Cambal, L., and Clougherty, J.: Examining the
451 transport of ammonia emissions across landscapes using nitrogen isotope ratios, *Atmos. Environ.*,
452 95, 563–570, <https://doi.org/10.1016/j.atmosenv.2014.06.061>, 2014.

453 Ferm, M.: Method for determination of atmospheric ammonia, *Atmospheric Environ.* 1967, 13,
454 1385–1393, [https://doi.org/10.1016/0004-6981\(79\)90107-0](https://doi.org/10.1016/0004-6981(79)90107-0), 1979.

455 Goebes, M. D., Strader, R., and Davidson, C.: An ammonia emission inventory for fertilizer
456 application in the United States, *Atmos. Environ.*, 37, 2539–2550, [https://doi.org/10.1016/S1352-](https://doi.org/10.1016/S1352-2310(03)00129-8)
457 2310(03)00129-8, 2003.

458 Groot Koerkamp, P. W. G., Metz, J. H. M., Uenk, G. H., Phillips, V. R., Holden, M. R., Sneath, R.
459 W., Short, J. L., White, R. P. P., Hartung, J., Seedorf, J., Schröder, M., Linkert, K. H., Pedersen, S.,
460 Takai, H., Johnsen, J. O., and Wathes, C. M.: Concentrations and emissions of ammonia in livestock
461 buildings in northern Europe, *J. Agric. Eng. Res.*, 70, 79–95, <https://doi.org/10.1006/jaer.1998.0275>,
462 1998.

463 Harrison, R. M. and Kitto, A.-M. N.: Field intercomparison of filter pack and denuder sampling
464 methods for reactive gaseous and particulate pollutants, *Atmospheric Environ. Part Gen. Top.*, 24,
465 2633–2640, [https://doi.org/10.1016/0960-1686\(90\)90142-A](https://doi.org/10.1016/0960-1686(90)90142-A), 1990.

466 Heaton, T. H. E.: Isotopic studies of nitrogen pollution in the hydrosphere and atmosphere: a review,
467 *Chem. Geol. Isot. Geosci. Sect.*, 59, 87–102, [https://doi.org/10.1016/0168-9622\(86\)90059-X](https://doi.org/10.1016/0168-9622(86)90059-X), 1986.

468 Hristov, A. N., Zaman, S., Vander Pol, M., Ndegwa, P., Campbell, L., and Silva, S.: Nitrogen losses
469 from dairy manure estimated through nitrogen mass balance and chemical markers, *J. Environ.*
470 *Qual.*, 38, 2438–2448, <https://doi.org/10.2134/jeq2009.0057>, 2009.

471 Huang, R.-J., Zhang, Y., Bozzetti, C., Ho, K.-F., Cao, J.-J., Han, Y., Daellenbach, K. R., Slowik, J.
472 G., Platt, S. M., Canonaco, F., Zotter, P., Wolf, R., Pieber, S. M., Brun, E. A., Crippa, M., Ciarelli,
473 G., Piazzalunga, A., Schwikowski, M., Abbaszade, G., Schnelle-Kreis, J., Zimmermann, R., An, Z.,
474 Szidat, S., Baltensperger, U., Haddad, I. E., and Prévôt, A. S. H.: High secondary aerosol
475 contribution to particulate pollution during haze events in China, *Nature*, 514, 218–222,
476 <https://doi.org/10.1038/nature13774>, 2014.

477 Huang, X., Song, Y., Li, M., Li, J., Huo, Q., Cai, X., Zhu, T., Hu, M., and Zhang, H.: A high-
478 resolution ammonia emission inventory in China, *Glob. Biogeochem. Cycles*, 26, 2011GB004161,
479 <https://doi.org/10.1029/2011GB004161>, 2012.

480 Jiang, H., Zhang, Q., Liu, W., Zhang, J., Pan, K., Zhao, T., and Xu, Z.: Isotopic compositions reveal
481 the driving forces of high nitrate level in an urban river: implications for pollution control, *J. Clean.*
482 *Prod.*, 298, 126693, <https://doi.org/10.1016/j.jclepro.2021.126693>, 2021.

483 Kawashima, H.: Seasonal trends of the stable nitrogen isotope ratio in particulate nitrogen
484 compounds and their gaseous precursors in akita, japan, *Tellus Ser. B-Chem. Phys. Meteorol.*, 71,
485 <https://doi.org/10.1080/16000889.2019.1627846>, 2019.

486 Kawashima, H. and Kurahashi, T.: Inorganic ion and nitrogen isotopic compositions of atmospheric
487 aerosols at yurihonjo, *Atmos. Environ.*, 45, 6309–6316,
488 <https://doi.org/10.1016/j.atmosenv.2011.08.057>, 2011.

489 Kawashima, H. and Ono, S.: Nitrogen isotope fractionation from ammonia gas to ammonium in
490 particulate ammonium chloride, *Environ. Sci. Technol.*, 53, 10629–10635,
491 <https://doi.org/10.1021/acs.est.9b01569>, 2019.

- 492 Kawashima, H., Yoshida, O., Joy, K. S., Raju, R. A., Islam, K. N., Jeba, F., and Salam, A.: Sources
493 identification of ammonium in PM_{2.5} during monsoon season in Dhaka, Bangladesh, *Sci. Total*
494 *Environ.*, 838, <https://doi.org/10.1016/j.scitotenv.2022.156433>, 2022.
- 495 Kawashima, H., Yoshida, O., and Suto, N.: Long-term source apportionment of ammonium in PM_{2.5}
496 at a suburban and a rural site using stable nitrogen isotopes, *Environ. Sci. Technol.*, 57, 1268–1277,
497 <https://doi.org/10.1021/acs.est.2c06311>, 2023.
- 498 Kirkby, J., Curtius, J., Almeida, J., Dunne, E., Duplissy, J., Ehrhart, S., Franchin, A., Gagné, S.,
499 Ickes, L., Kürten, A., Kupc, A., Metzger, A., Riccobono, F., Rondo, L., Schobesberger, S.,
500 Tsagkogeorgas, G., Wimmer, D., Amorim, A., Bianchi, F., Breitenlechner, M., David, A., Dommen,
501 J., Downard, A., Ehn, M., Flagan, R. C., Haider, S., Hansel, A., Hauser, D., Jud, W., Junninen, H.,
502 Kreissl, F., Kvashin, A., Laaksonen, A., Lehtipalo, K., Lima, J., Lovejoy, E. R., Makhmutov, V.,
503 Mathot, S., Mikkilä, J., Minginette, P., Mogo, S., Nieminen, T., Onnela, A., Pereira, P., Petäjä, T.,
504 Schnitzhofer, R., Seinfeld, J. H., Sipilä, M., Stozhkov, Y., Stratmann, F., Tomé, A., Vanhanen, J.,
505 Viisanen, Y., Vrtala, A., Wagner, P. E., Walther, H., Weingartner, E., Wex, H., Winkler, P. M., Carslaw,
506 K. S., Worsnop, D. R., Baltensperger, U., and Kulmala, M.: Role of sulphuric acid, ammonia and
507 galactic cosmic rays in atmospheric aerosol nucleation, *Nature*, 476, 429–433,
508 <https://doi.org/10.1038/nature10343>, 2011.
- 509 Leng, Q., Cui, J., Zhou, F., Du, K., Zhang, L., Fu, C., Liu, Y., Wang, H., Shi, G., Gao, M., Yang, F.,
510 and He, D.: Wet-only deposition of atmospheric inorganic nitrogen and associated isotopic
511 characteristics in a typical mountain area, southwestern China, *Sci. Total Environ.*, 616, 55–63,
512 <https://doi.org/10.1016/j.scitotenv.2017.10.240>, 2018.
- 513 Li, K., Xu, D., Zhang, L., Liu, W., Zhan, M., Su, Y., Wu, D., and Xie, B.: Integrated isotopic labeling
514 analysis unveils precise proportions of ammonia emissions during composting, *J. Clean. Prod.*, 450,
515 141799, <https://doi.org/10.1016/j.jclepro.2024.141799>, 2024.
- 516 Li, T., Wang, C., Ji, W., Wang, Z., Shen, W., Feng, Y., and Zhou, M.: Cutting-edge ammonia
517 emissions monitoring technology for sustainable livestock and poultry breeding: a comprehensive
518 review of the state of the art, *J. Clean. Prod.*, 428, 139387,
519 <https://doi.org/10.1016/j.jclepro.2023.139387>, 2023a.
- 520 Li, T., Li, J., Sun, Z., Jiang, H., Tian, C., and Zhang, G.: High contribution of anthropogenic
521 combustion sources to atmospheric inorganic reactive nitrogen in south China evidenced by isotopes,
522 *Atmospheric Chem. Phys.*, 23, 6395–6407, <https://doi.org/10.5194/acp-23-6395-2023>, 2023b.
- 523 Lim, S., Lee, M., Czimczik, C. I., Joo, T., Holden, S., Mouteva, G., Santos, G. M., Xu, X., Walker,
524 J., Kim, S., Kim, H. S., Kim, S., and Lee, S.: Source signatures from combined isotopic analyses of
525 PM_{2.5} carbonaceous and nitrogen aerosols at the peri-urban taehwa research forest, South Korea in
526 summer and fall, *Sci. Total Environ.*, 655, 1505–1514,
527 <https://doi.org/10.1016/j.scitotenv.2018.11.157>, 2019.
- 528 Lim, S., Hwang, J., Lee, M., Czimczik, C. I., Xu, X., and Savarino, J.: Robust evidence of ¹⁴C,
529 ¹³C, and ¹⁵N analyses indicating fossil fuel sources for total carbon and ammonium in fine aerosols

530 in Seoul megacity, *Environ. Sci. Technol.*, 56, 6894–6904, <https://doi.org/10.1021/acs.est.1c03903>,
531 2022.

532 Liu, D., Quan, Z., Wang, Y., Huang, K., Zhang, Q., Song, L., Huang, S., Wang, Y., Xun, Z., Liu, D.,
533 Liu, C., Fang, Y., and Sun, J.: Investigating the effects of animal-specific $\delta^{15}\text{N-NH}_3$ values
534 volatilized from livestock waste on regional NH_3 source partitioning, *Atmospheric Environ. X*, 25,
535 100314, <https://doi.org/10.1016/j.aeaoa.2025.100314>, 2025.

536 Liu, M., Huang, X., Song, Y., Tang, J., Cao, J., Zhang, X., Zhang, Q., Wang, S., Xu, T., Kang, L.,
537 Cai, X., Zhang, H., Yang, F., Wang, H., Yu, J. Z., Lau, A. K. H., He, L., Huang, X., Duan, L., Ding,
538 A., Xue, L., Gao, J., Liu, B., and Zhu, T.: Ammonia emission control in China would mitigate haze
539 pollution and nitrogen deposition, but worsen acid rain, *Proc. Natl. Acad. Sci.*, 116, 7760–7765,
540 <https://doi.org/10.1073/pnas.1814880116>, 2019.

541 Liu, X., Zhang, Y., Han, W., Tang, A., Shen, J., Cui, Z., Vitousek, P., Erisman, J. W., Goulding, K.,
542 Christie, P., Fangmeier, A., and Zhang, F.: Enhanced nitrogen deposition over china, *Nature*, 494,
543 459–462, <https://doi.org/10.1038/nature11917>, 2013.

544 Ma, R., Zou, J., Han, Z., Yu, K., Wu, S., Li, Z., Liu, S., Niu, S., Horwath, W. R., and Zhu-Barker,
545 X.: Global soil-derived ammonia emissions from agricultural nitrogen fertilizer application: a
546 refinement based on regional and crop-specific emission factors, *Glob. Change Biol.*, 27, 855–867,
547 <https://doi.org/10.1111/gcb.15437>, 2021.

548 Meng, W., Zhong, Q., Yun, X., Zhu, X., Huang, T., Shen, H., Chen, Y., Chen, H., Zhou, F., Liu, J.,
549 Wang, X., Zeng, E. Y., and Tao, S.: Improvement of a global high-resolution ammonia emission
550 inventory for combustion and industrial sources with new data from the residential and
551 transportation sectors, *Environ. Sci. Technol.*, 51, 2821–2829,
552 <https://doi.org/10.1021/acs.est.6b03694>, 2017.

553 Pan, Y., Tian, S., Liu, D., Fang, Y., Zhu, X., Gao, M., Wentworth, G. R., Michalski, G., Huang, X.,
554 and Wang, Y.: Source apportionment of aerosol ammonium in an ammonia-rich atmosphere: an
555 isotopic study of summer clean and hazy days in urban beijing, *J. Geophys. Res. Atmospheres*, 123,
556 5681–5689, <https://doi.org/10.1029/2017JD028095>, 2018.

557 Pan, Y., Gu, M., Song, L., Tian, S., Wu, D., Walters, W. W., Yu, X., Lü, X., Ni, X., Wang, Y., Cao,
558 J., Liu, X., Fang, Y., and Wang, Y.: Systematic low bias of passive samplers in characterizing
559 nitrogen isotopic composition of atmospheric ammonia, *Atmospheric Res.*, 243, 105018–105025,
560 <https://doi.org/10.1016/j.atmosres.2020.105018>, 2020.

561 Parnell, A. C., Inger, R., Bearhop, S., and Jackson, A. L.: Source partitioning using stable isotopes:
562 coping with too much variation, *PLOS One*, 5, e9672, <https://doi.org/10.1371/journal.pone.0009672>,
563 2010.

564 Qu, Q. and Zhang, K.: Effects of pH, total solids, temperature and storage duration on gas emissions
565 from slurry storage: a systematic review, *Atmosphere*, 12, 1156,
566 <https://doi.org/10.3390/atmos12091156>, 2021.

567 Rosa, E., Arriaga, H., and Merino, P.: Ammonia emission from a manure-belt laying hen facility
568 equipped with an external manure drying tunnel, *J. Clean. Prod.*, 251, 119591,
569 <https://doi.org/10.1016/j.jclepro.2019.119591>, 2020.

570 Ryu, H.-D., Kim, S.-J., Baek, U., Kim, D.-W., Lee, H.-J., Chung, E. G., Kim, M.-S., Kim, K., and
571 Lee, J. K.: Identifying nitrogen sources in intensive livestock farming watershed with swine excreta
572 treatment facility using dual ammonium ($\delta^{15}\text{NNH}_4$) and nitrate ($\delta^{15}\text{NNO}_3$) nitrogen isotope ratios
573 axes, *Sci. Total Environ.*, 779, 146480, <https://doi.org/10.1016/j.scitotenv.2021.146480>, 2021.

574 Savard, M. M., Cole, A., Smirnoff, A., and Vet, R.: $\delta^{15}\text{N}$ values of atmospheric N species
575 simultaneously collected using sector-based samplers distant from sources – isotopic inheritance
576 and fractionation, *Atmos. Environ.*, 162, 11–22, <https://doi.org/10.1016/j.atmosenv.2017.05.010>,
577 2017.

578 Schlesinger, William H. and Hartley, Anne E.: A global budget for atmospheric NH_3 ,
579 *Biogeochemistry*, 15, <https://doi.org/10.1007/bf00002936>, 1992.

580 Skinner, R., Ineson, P., Jones, H., Sleep, D., and Theobald, M.: Sampling systems for isotope-ratio
581 mass spectrometry of atmospheric ammonia, *Rapid Commun. Mass Spectrom.*, 20, 81–88,
582 <https://doi.org/10.1002/rcm.2279>, 2006.

583 Soler-Jofra, A., Stevens, B., Hoekstra, M., Picioreanu, C., Sorokin, D., Van Loosdrecht, M. C. M.,
584 and Pérez, J.: Importance of abiotic hydroxylamine conversion on nitrous oxide emissions during
585 nitrification of reject water, *Chem. Eng. J.*, 287, 720–726, <https://doi.org/10.1016/j.cej.2015.11.073>,
586 2016.

587 Song, L., Walters, W. W., Pan, Y., Li, Z., Gu, M., Duan, Y., Lü, X., and Fang, Y.: ^{15}N natural
588 abundance of vehicular exhaust ammonia, quantified by active sampling techniques, *Atmos.*
589 *Environ.*, 255, 118430–118440, <https://doi.org/10.1016/j.atmosenv.2021.118430>, 2021.

590 Song, L., Wang, A., Li, Z., Kang, R., Walters, W. W., Pan, Y., Quan, Z., Huang, S., and Fang, Y.:
591 Large seasonal variation in nitrogen isotopic abundances of ammonia volatilized from a cropland
592 ecosystem and implications for regional NH_3 source partitioning, *Environ. Sci. Technol.*, 58, 1177–
593 1186, <https://doi.org/10.1021/acs.est.3c08800>, 2024.

594 Stock, B. C. and Semmens, B. X.: Unifying error structures in commonly used biotracer mixing
595 models, *Ecology*, 97, 2562–2569, <https://doi.org/10.1002/ecy.1517>, 2016.

596 Stratton, J. J., Ham, J., Collett, J. L., Jr., Benedict, K., and Borch, T.: Assessing the efficacy of
597 nitrogen isotopes to distinguish Colorado front range ammonia sources affecting Rocky Mountain
598 National Park, *Atmos. Environ.*, 215, <https://doi.org/10.1016/j.atmosenv.2019.116881>, 2019.

599 Streets, D. G., Bond, T. C., Carmichael, G. R., Fernandes, S. D., Fu, Q., He, D., Klimont, Z., Nelson,
600 S. M., Tsai, N. Y., Wang, M. Q., Woo, J.-H., and Yarber, K. F.: An inventory of gaseous and primary
601 aerosol emissions in Asia in the year 2000, *J. Geophys. Res. Atmospheres*, 108,
602 <https://doi.org/10.1029/2002JD003093>, 2003.

603 Sui, Y., Ou, Y., Yan, B., Rousseau, A. N., Fang, Y., Geng, R., Wang, L., and Ye, N.: A dual isotopic
604 framework for identifying nitrate sources in surface runoff in a small agricultural watershed,
605 northeast China, *J. Clean. Prod.*, 246, 119074, <https://doi.org/10.1016/j.jclepro.2019.119074>, 2020.

606 Ti, C., Gao, B., Luo, Y., Wang, X., Wang, S., and Yan, X.: Isotopic characterization of $\text{NH}_x\text{-N}$ in
607 deposition and major emission sources, *Biogeochemistry*, 138, 85–102,
608 <https://doi.org/10.1007/s10533-018-0432-3>, 2018.

609 Ti, C., Xia, L., Chang, S. X., and Yan, X.: Potential for mitigating global agricultural ammonia
610 emission: A meta-analysis, *Environ. Pollut.*, 245, 141–148,
611 <https://doi.org/10.1016/j.envpol.2018.10.124>, 2019.

612 Ti, C., Ma, S., Peng, L., Tao, L., Wang, X., Dong, W., Wang, L., and Yan, X.: Changes of $\delta^{15}\text{N}$
613 values during the volatilization process after applying urea on soil, *Environ. Pollut.*, 270, 116204,
614 <https://doi.org/10.1016/j.envpol.2020.116204>, 2021.

615 Van Damme, M., Clarisse, L., Whitburn, S., Hadji-Lazaro, J., Hurtmans, D., Clerbaux, C., and
616 Coheur, P.-F.: Industrial and agricultural ammonia point sources exposed, *Nature*, 564, 99–103,
617 <https://doi.org/10.1038/s41586-018-0747-1>, 2018.

618 Walters, W. W., Karod, M., Willcocks, E., Baek, B. H., Blum, D. E., and Hastings, M. G.:
619 Quantifying the importance of vehicle ammonia emissions in an urban area of northeastern USA
620 utilizing nitrogen isotopes, *Atmospheric Chem. Phys.*, 22, 13431–13448,
621 <https://doi.org/10.5194/acp-22-13431-2022>, 2022.

622 Wang, C., Yin, S., Bai, L., Zhang, X., Gu, X., Zhang, H., Lu, Q., and Zhang, R.: High-resolution
623 ammonia emission inventories with comprehensive analysis and evaluation in henan, china, 2006–
624 2016, *Atmos. Environ.*, 193, 11–23, <https://doi.org/10.1016/j.atmosenv.2018.08.063>, 2018.

625 Wang, C., Li, X., Zhang, T., Tang, A., Cui, M., Liu, X., Ma, X., Zhang, Y., Liu, X., and Zheng, M.:
626 Developing nitrogen isotopic source profiles of atmospheric ammonia for source apportionment of
627 ammonia in urban beijing, *Front. Environ. Sci.*, 10, <https://doi.org/10.3389/fenvs.2022.903013>,
628 2022.

629 Warner, J. X., Dickerson, R. R., Wei, Z., Strow, L. L., Wang, Y., and Liang, Q.: Increased
630 atmospheric ammonia over the world’s major agricultural areas detected from space, *Geophys. Res.*
631 *Lett.*, 44, 2875–2884, <https://doi.org/10.1002/2016gl072305>, 2017.

632 Wong, W. W., Cartwright, I., Poh, S. C., and Cook, P.: Sources and cycling of nitrogen revealed by
633 stable isotopes in a highly populated large temperate coastal embayment, *Sci. Total Environ.*, 806,
634 150408, <https://doi.org/10.1016/j.scitotenv.2021.150408>, 2022.

635 Wu, L., Ren, H., Wang, P., Chen, J., Fang, Y., Hu, W., Ren, L., Deng, J., Song, Y., Li, J., Sun, Y.,
636 Wang, Z., Liu, C.-Q., Ying, Q., and Fu, P.: Aerosol ammonium in the urban boundary layer in beijing:
637 insights from nitrogen isotope ratios and simulations in summer 2015, *Environ. Sci. Technol. Lett.*,
638 6, 389–395, <https://doi.org/10.1021/acs.estlett.9b00328>, 2019.

639 Wu, L., Zhang, Y., Xiao, Y., Zhu, J., Shi, Z., Wang, Y., Xu, H., Hu, W., Deng, J., Tang, M., and Fu,
640 P.: Diversity of ammonia sources in tianjin: nitrogen isotope analyses and simulations of aerosol
641 ammonium, *Environ. Chem.* 14482517, 21, 1–13, <https://doi.org/10.1071/EN24030>, 2024.

642 Xi, D., Xiao, Y., Mgelwa, A. S., and Kuang, Y.: Formation pathways and source apportionments of
643 inorganic nitrogen-containing aerosols in urban environment: insights from nitrogen and oxygen
644 isotopic compositions in guangzhou, china, *Atmos. Environ.*, 309,
645 <https://doi.org/10.1016/j.atmosenv.2023.119888>, 2023.

646 Xiang, Y.-K., Dao, X., Gao, M., Lin, Y.-C., Cao, F., Yang, X.-Y., and Zhang, Y.-L.: Nitrogen isotope
647 characteristics and source apportionment of atmospheric ammonium in urban cities during a haze
648 event in northern China plain, *Atmos. Environ.*, 269, 118800–118813,
649 <https://doi.org/10.1016/j.atmosenv.2021.118800>, 2022.

650 Xiao, H., Ding, S.-Y., Ji, C.-W., Li, Q.-K., and Li, X.-D.: Combustion related ammonia promotes
651 PM_{2.5} accumulation in autumn in tianjin, china, *Atmospheric Res.*, 275,
652 <https://doi.org/10.1016/j.atmosres.2022.106225>, 2022.

653 Xiao, H., Xiao, H.-W., Xu, Y., Zheng, N.-J., and Xiao, H.-Y.: Combustion-driven inorganic nitrogen
654 in PM_{2.5} from a city in central china has the potential to enhance the nitrogen load of north China,
655 *J. Hazard. Mater.*, 483, <https://doi.org/10.1016/j.jhazmat.2024.136620>, 2025.

656 Xiao, H.-W., Wu, J.-F., Luo, L., Liu, C., Xie, Y.-J., and Xiao, H.-Y.: Enhanced biomass burning as
657 a source of aerosol ammonium over cities in central China in autumn, *Environ. Pollut.*, 266, 115278,
658 <https://doi.org/10.1016/j.envpol.2020.115278>, 2020.

659 Xie, Y., Xiong, Z., Xing, G., Yan, X., Shi, S., Sun, G., and Zhu, Z.: Source of nitrogen in wet
660 deposition to a rice agroecosystem at tai lake region, *Atmos. Environ.*, 42, 5182–5192,
661 <https://doi.org/10.1016/j.atmosenv.2008.03.008>, 2008.

662 Xu, P., Li, G., Zheng, Y., Fung, J. C. H., Chen, A., Zeng, Z., Shen, H., Hu, M., Mao, J., Zheng, Y.,
663 Cui, X., Guo, Z., Chen, Y., Feng, L., He, S., Zhang, X., Lau, A. K. H., Tao, S., and Houlton, B. Z.:
664 Fertilizer management for global ammonia emission reduction, *Nature*, 626, 792–798,
665 <https://doi.org/10.1038/s41586-024-07020-z>, 2024.

666 Yang, F., Tan, J., Zhao, Q., Du, Z., He, K., Ma, Y., Duan, F., Chen, G., and Zhao, Q.: Characteristics
667 of PM_{2.5} speciation in representative megacities and across china, *Atmospheric Chem. Phys.*, 11,
668 5207–5219, <https://doi.org/10.5194/acp-11-5207-2011>, 2011.

669 Zhang, H., Hong, Z., Wei, L., Thornton, B., Hong, Y., Chen, J., and Zhang, X.: Stable isotopes
670 unravel the sources and transport of PM_{2.5} in the Yangtze River delta, china, *Atmosphere*, 14,
671 <https://doi.org/10.3390/atmos14071120>, 2023.

672 Zhang, L., Altabet, M. A., Wu, T., and Hadas, O.: Sensitive measurement of NH₄⁺ ¹⁵N/¹⁴N
673 ($\delta^{15}\text{NH}_4^+$) at natural abundance levels in fresh and saltwaters, *Anal. Chem.*, 79, 5297–5303,
674 <https://doi.org/10.1021/ac070106d>, 2007.

675 Zhou, Y., Zheng, N., Luo, L., Zhao, J., Qu, L., Guan, H., Xiao, H., Zhang, Z., Tian, J., and Xiao, H.:
676 Biomass burning related ammonia emissions promoted a self-amplifying loop in the urban
677 environment in kunming (SW china), *Atmos. Environ.*, 253,
678 <https://doi.org/10.1016/j.atmosenv.2020.118138>, 2021.

679 Zou, D., Sun, Q., Liu, J., Xu, C., and Song, S.: Seasonal source analysis of nitrogen and carbon
680 aerosols of PM_{2.5} in typical cities of zhejiang, china, *Chemosphere*, 303,
681 <https://doi.org/10.1016/j.chemosphere.2022.135026>, 2022.

682